A hybrid particle–field molecular dynamics approach: a route toward efficient coarse-grained models for biomembranes

2013 Phys. Biol. 10 045007

(http://iopscience.iop.org/1478-3975/10/4/045007)

Phys. Biol. **10** (2013) 045007 (16pp) doi:10.1088/1478-3975/10/4/045007

A hybrid particle–field molecular dynamics approach: a route toward efficient coarse-grained models for biomembranes

Giuseppe Milano[1,2], **Toshihiro Kawakatsu**[3] **and Antonio De Nicola**[1,2]

[1] Dipartimento di Chimica e Biologia, Università di Salerno, I-84084 via Ponte don Melillo Fisciano (SA), Italy
[2] IMAST Scarl-Technological District in Polymer and Composite Engineering, P.le Bovio 22, I-80133 Napoli (NA), Italy
[3] Department of Physics, Tohoku University, Aoba, Aramaki, Aoba-ku, Sendai 980-8578, Japan

E-mail: gmilano@unisa.it

Received 7 January 2013
Accepted for publication 17 May 2013
Published 2 August 2013
Online at stacks.iop.org/PhysBio/10/045007

Abstract
This paper gives an overview of the coarse-grained models of phospholipids recently developed by the authors in the frame of a hybrid particle–field molecular dynamics technique. This technique employs a special class of coarse-grained models that are gaining popularity because they allow simulations of large scale systems and, at the same time, they provide sufficiently detailed chemistry for the mapping scheme adopted. The comparison of the computational costs of our approach with standard molecular dynamics simulations is a function of the system size and the number of processors employed in the parallel calculations. Due to the low amount of data exchange, the larger the number of processors, the better are the performances of the hybrid particle–field models. This feature makes these models very promising ones in the exploration of several problems in biophysics.

1. Introduction

Simulation approaches aimed at accessing long time and length scales are relevant for a successful modeling strategy. In particular, these approaches are suitable for the typical problems of molecular crowding and more generally for biomolecular processes. Molecular dynamics (MD) simulations for the study of these processes have been performed for a long time [1–4]. However, these simulations are still computationally very expensive when studying processes occurring on the mesoscopic time ($>\mu$s) and length scales ($>$100 nm). Therefore, to overcome this problem, alternative computational methods aiming to bridge the time and length scales involved in the relevant phenomena are constantly being proposed [5–7].

Among the several types of biomolecules, phospholipids are an important class. When they are in water their amphiphilic structure allows them to self-assemble into a lipid bilayer with lipid tails shielded from the water and polar head groups exposed to the polar environment. In living organisms, lipid bilayers form cellular membranes. Biological membranes are very complex systems and macromolecular crowding at membrane interfaces has been studied using model peptides, which upon membrane adsorption can adopt peculiar transmembrane, as well as in-planar, configurations [8].

The aim of this paper is to give an overview of the coarse-grained (CG) models of phospholipids that have recently been developed by the authors in the frame of a hybrid particle–field MD technique. This technique employs a special class of CG model that are gaining popularity because they allow simulations of large scale systems using a reasonable amount of computational resources and are useful when approaching the problems of complex biomolecular systems.

The paper is organized as follows. Section 2 is devoted to a brief overview of CG models of phospholipids. In section 3

the basics of the hybrid particle–field MD technique and its implementation for parallel architecture is reviewed. In section 4 the description of the models, their validation and the main results are reviewed.

2. Coarse-grained models of phospholipids

For their relevance in biology, lipid bilayers have attracted the attention of the computational biophysics community. Recently, CG simulations have become a very popular method for the study of these systems. The CG approach exploits the reduction of the degrees of freedom in the atomic model of the simulated system by combining several atoms into a single particle ('effective bead'). CG methods have been successfully used to approach several problems involving polymers [9–11], biomolecules [12–15] and more generally soft matter [16, 17].

For phospholipids, different types of CG models have been developed. For a complete overview, the reader should refer to a number of recent reviews [6, 12–15]. Starting from Smit's [18] seminal study, in which an off-lattice CG model for lipids and water was introduced, several CG models have since been developed. Sintes and Baumgärtner [19, 20] developed a CG model for lipid bilayers where the solvent was taken into account implicitly. Later, Lenz and Schmid extended the implicit-solvent model to pure lipid bilayers composed of saturated lipids [21]. Goetz and Lipowsky introduced an explicit-solvent CG model for lipid membranes where a binary Lennard-Jones fluid for the solvent and a short chain of beads for the amphiphilic molecules were used [22].

The degree of coarse-graining of a model is related to the type of process that one wants to investigate. CG models having a low discrimination of the chemical details of the molecule can be successfully applied to study self-assembly phenomena involving many molecules when the microscopic chemical structures of the constituent molecules are expected to be irrelevant for the process; systems can only be described by a small number of key properties, e.g., the amphiphilic nature of the molecules. Usually for membrane systems, the clear separation in length, time and energy scales assumed in this approach is often missing and the chemical specificity of the target systems needs to be taken into account in the models. Furthermore, these simple models can fail to reproduce more complex phenomena involving specific interactions of the membrane with other biomolecules (e.g. proteins or peptides). In these cases, the nature of the CG models limits their application range.

To avoid these drawbacks, CG models that provide sufficiently detailed chemistry have been built. These CG models usually employ several different types of beads (not just hydrophobic and hydrophilic) referring to specific groups of atoms; in the literature there are several examples of such models [18, 23–29]. A widely explored example of this approach is the MARTINI model developed by Marrink *et al* [30]. The phospholipids in the MARTINI model are described by beads having different Lennard-Jones type interaction parameters that can smoothly modulate their hydrophobic/hydrophilic character. Furthermore, water molecules are treated explicitly with a CG reduction scheme of four molecules to one. Despite its apparent simplicity, the MARTINI force field is, with fairly good accuracy, able to reproduce the properties of self-assembled lipid bilayers [31–33]. In particular, the mapping scheme adopted in the MARTINI model is close to atomistic models, consisting of beads each of which represents a few atoms (usually 3 atoms in one bead, 3:1 mapping): the MARTINI model enables the study of specific phospholipids and the effect of various molecules on membranes (for instance butanol [34], DMSO [35], dendrimers [36] and proteins [37]). On the other hand, computational approaches based on different representations (fields) have been proposed to model soft matter problems. In particular, in the frame of the self-consistent field (SCF) theory, the model systems are not represented by particles but by density fields; the mutual interactions between segments are decoupled and replaced by an interaction between the segments and static external fields [38]. The external fields in the SCF theory depend on the statistical average of the spatially inhomogeneous density distributions of the segments of independent molecules, which only interact through these fields. Such external fields and their particle density distributions have to be determined self-consistently. Numerous applications to block copolymers [39–42], proteins [43], polymer composites [44] and colloidal particles [45, 46] have shown that the SCF theory is a useful and powerful method.

Several studies have been reported in literature to study mixtures of phospholipids and water using a field-based approach. The first field model of lipid molecules was proposed by Marcelja [47]. According to Marcelja's model, the head groups of the lipid molecules are modeled using a boundary to which the tails of the lipid molecules are anchored. The degrees of freedom corresponding to intra-molecular rearrangement are sampled using the rotational isomeric state (RIS) model, where the segments are coupled through an anisotropic aligning potential [47]. The inequivalence of the tail, head and solvent segments allows one to describe the bilayers as pre-assembled structures; it does not allow for the study of self-assembly. A fully self-consistent approach capable of describing stable, tensionless, self-assembled bilayers was introduced later. Both random-chain and the RIS-chain model result in membranes with qualitatively similar segment distributions and with similar thermodynamic properties [48]. Quantitatively, however, this approach underestimates the experimentally measured membrane thickness by about 50% [6].

More recently, molecular-level SCF theories that are able to describe phospholipids have been developed [6]. The main idea of these SCF techniques is to split up the calculation of multibody interactions in two procedures: i.e. to find the ensemble averaged conformation distribution and to find the segment potentials based on the segment distribution. For this aim, a set of partial differential equations are solved numerically using lattice approximations and a discrete set of coordinates, onto which segments can be placed, has to be defined. Layers are kept imposing reflecting boundary conditions to assure multilamellar system. Parameters are defined so that the results of the MD simulations are

reproduced by those of the SCF simulations [48]. Müller and Schick [49] proposed a novel approach developing an off-lattice representation of the field theory; they obtained the single-chain partition function via a partial enumeration [50] over a large set of molecular conformations of a lipid chain with RIS statistics. Also in the case of a single lipid in an external field, as the partition function cannot be obtained analytically for a realistic molecular architecture, one has to approximate the probability distributions of the conformations of non-interacting lipid molecules by a representative sample of single lipid conformations.

More recently, the single chain in mean field (SCMF) method introduced by Müller *et al*, in which a density field is kept static for a number of Monte Carlo steps, has been successfully applied to homopolymer and block copolymer systems [51–53].

One of the advantages of this hybrid approach is the lack of any limitation in treating complex molecular architectures and/or intramolecular interactions. In the frame of the hybrid scheme proposed by Müller, this approach has recently been extended to molecular dynamics (MD) simulations. In particular, the MD method has been combined with SCF description (MD-SCF); an implementation suitable for the treatment of atomistic force fields and/or specific CG models has been reported and validated [54, 55].

Particle based CG models like MARTINI are still computationally demanding when compared to SCF approaches. On the other hand, SCF approaches assure accessibility to larger length and time scales but at the cost of very low chemical specificity. The idea behind the combined MD-SCF method and the corresponding lipid models is to obtain a strategy, as far as is possible, having the main advantages and avoiding the main disadvantages of the SCF and MD techniques. After the introduction of the MD-SCF approach, this kind of hybrid model, due to its computational efficiency (quantitative comparisons between the computational costs of SCF approaches, hybrid particle–field and standard MD simulations are reported in section 3.4), is also gaining popularity for biomembranes modeling. In particular, a solvent-free CG model for lipid bilayer membranes, where non-bonded interactions were treated by a weighted-density functional, has been introduced by Hömberg and Müller [56]. Very recently, Sevink *et al* introduced a hybrid scheme, combining Brownian dynamics (BD) and dynamic density functional theory (DDFT), that is able to model efficiently complete vesicles with molecular detail [57].

In the following the basic theoretical scheme of MD-SCF simulations and its implementation also for parallel computer architectures will be described.

3. Hybrid particle–field molecular dynamics

3.1. Theoretical scheme

In this section, a description of the hybrid particle–field MD simulation scheme is given. For further details and a complete treatment of this approach the readers can refer to [33, 34] where the derivation and the implementation have been introduced and to [38, 58] for a general aspect of SCF methods.

According to the spirit of SCF theory, the main approach of the hybrid particle–field method is to reduce a many body problem, like molecular motion in many particle systems, to the problem of deriving the partition function of a single molecule in an external potential $V(\mathbf{r})$ and to obtain a suitable expression of the $V(\mathbf{r})$ and its derivatives. In this way the evaluation of the forces between non-bonded atoms and the potential between atoms of different molecules, i.e. the most computationally expensive part of MD simulations, is reformulated as an evaluation of the external potential that depends on the local density at the atomic positions.

A molecule in SCF theory is considered to be interacting with the neighboring molecules not directly but only through an averaged density field. The Hamiltonian of a system composed of M molecules, according to this picture, can be split into two parts as $\hat{H}(\Gamma) = \hat{H}_0(\Gamma) + \hat{W}(\Gamma)$. Assuming the canonical ensemble (*NVT*-ensemble), the partition function of this system is:

$$Z = \frac{1}{M!}\int \mathrm{d}\Gamma \exp\{-\beta[\hat{H}_0(\Gamma) + \hat{W}(\Gamma)]\}, \tag{1}$$

where Γ is used as shorthand for a set of positions of all atoms in the system, which specifies a point in the phase space. In equation (1) and also in the following, the symbol ˆ (hat) indicates that the associated physical quantity is a function of the microscopic states described by the phase space Γ. $\hat{H}_0(\Gamma)$ is the Hamiltonian of a reference ideal system composed of M non-interacting chains but with all the intramolecular interaction terms (bond, angle, etc) that are taken into account in the same way as in the standard MD simulations. On the other hand, the deviation from the reference system due to the intermolecular non-bonded interactions is accounted for by the term $\hat{W}(\Gamma)$ in equation (1).

The microscopic density, i.e. the density distribution of atoms as a function of the positions of point particles, can be defined as a sum of delta-functions centered at the center of mass of each particle as:

$$\hat{\phi}(\mathbf{r}, \Gamma) = \sum_{p=1}^{M}\sum_{i=0}^{N(p)} \delta\left(\mathbf{r} - \mathbf{r}_i^{(p)}\right), \tag{2}$$

where $\mathbf{r}_i^{(p)}$ is the position of the ith particle belonging to the pth molecule and $N(p)$ is the number of particles contained in the pth molecule.

The deviation $\hat{W}(\Gamma)$ from the reference state $\hat{H}_0$, according to equation (1), originates from the interactions between molecules. To evaluate this interaction term $\hat{W}(\Gamma)$, several assumptions can be introduced. The first assumption is that $\hat{W}(\Gamma)$ depends on Γ but not directly and only through the particle density $\hat{\phi}(\mathbf{r};\Gamma)$ as:

$$\hat{W}(\Gamma) = W[\hat{\phi}(\mathbf{r}, \Gamma)], \tag{3}$$

where $W[\hat{\phi}]$ is a functional of $\hat{\phi}(\mathbf{r}, \Gamma)$.

Under this assumption and using the definition of δ-functional, the partition function in equation (1) can be rewritten as:

$$Z = \frac{1}{M!}\int D\{\varphi(\mathbf{r})\}\int D\{w(\mathbf{r})\}\exp\left\{-\beta\left[-\frac{M}{\beta}\ln z + W[\varphi(\mathbf{r})] - \int \mathrm{d}\mathbf{r}\, V(\mathbf{r})\varphi(\mathbf{r})\right]\right\} \quad (4)$$

where $w(\mathbf{r})$ is a conjugate field of $\varphi(\mathbf{r})$ that appeared in the Fourier representation of the δ-functional and z is the partition function of a single molecule in an external potential $V(\mathbf{r})$ defined as:

$$z[V(\mathbf{r})] = \int \mathrm{d}\Gamma_1 \exp\left[-\beta\left\{\hat{h}_0(\Gamma_1) + \sum_i V(\mathbf{r}_i)\right\}\right], \quad (5)$$

where $\Gamma_1 \equiv \{r_i\}$ is the phase space of a single molecule and $\hat{h}_0(\Gamma_1)$ is the Hamiltonian of an isolated molecule.

A mean field approximation, in terms of this partition function, can be obtained by replacing the integrals over $\varphi(\mathbf{r})$ and $w(\mathbf{r})$ in equation (5) with a Gaussian integral around the most probable state, which minimizes the argument of the exponential function on the right-hand side of equation (4) (so-called saddle point approximation).

The conditions of such a minimization in the form of functional derivatives give the following:

$$\begin{cases} V(\mathbf{r}) = \dfrac{\delta W[\varphi(\mathbf{r})]}{\delta\varphi(\mathbf{r})} \\ \varphi(\mathbf{r}) = -\dfrac{M}{\beta z}\dfrac{\delta z}{\delta V(\mathbf{r})} = \langle\hat{\phi}(\mathbf{r};\Gamma)\rangle \equiv \phi(\mathbf{r}) \end{cases}. \quad (6)$$

Using equation (6), it is possible to obtain an expression for the density dependent external potential acting on each molecule.

Now we extend the above formulation to multi-component systems. In such a case, the interaction term W, where each component species is specified by an index K, is assumed to have the following form

$$W[\{\phi_K(\mathbf{r})\}] = \int \mathrm{d}\mathbf{r}\left(\frac{k_B T}{2}\sum_{KK'}\phi_K(\mathbf{r})\phi_{K'}(\mathbf{r}) + \frac{1}{2\kappa}\left(\sum_K \phi_K(\mathbf{r}) - 1\right)^2\right), \quad (7)$$

where the second term of the integrand on the right-hand side is the relaxed incompressibility condition, ϕ_0 is the total number density of segments (we assume the same volume for all segment species) and κ is the compressibility that is assumed to be sufficiently small. Then, the corresponding mean field potential acting on the K-species is given by

$$V_K(\mathbf{r}) = \frac{\delta W[\{\phi_K(\mathbf{r})\}]}{\delta\phi_K(\mathbf{r})} = k_B T\sum_{K'}\chi_{KK'}\phi_{K'}(\mathbf{r}) + \frac{1}{\kappa}\left(\sum_K \phi_K(\mathbf{r}) - 1\right). \quad (8)$$

Let us give a simple example, i.e. a case of a mixture of two components A and B. In this case the mean field potential acting on a segment of type A at position $\mathbf{r}$ is given by:

$$V_A(\mathbf{r}) = k_B T[\chi_{AA}\phi_A(\mathbf{r}) + \chi_{AB}\phi_B(\mathbf{r})] + \frac{1}{\kappa}(\phi_A(\mathbf{r}) + \phi_B(\mathbf{r}) - 1). \quad (9)$$

The force acting on segment A at position $\mathbf{r}$ imposed by the interaction with the density field is:

$$F_A(\mathbf{r}) = -\frac{\partial V_A(\mathbf{r})}{\partial\mathbf{r}} = -k_B T\left(\chi_{AA}\frac{\partial V_A(\mathbf{r})}{\partial\mathbf{r}} + \chi_{AB}\frac{\partial\phi_B(\mathbf{r})}{\partial\mathbf{r}}\right) - \frac{1}{\kappa}\left(\frac{\partial\phi_A(\mathbf{r})}{\partial\mathbf{r}} + \frac{\partial\phi_B(\mathbf{r})}{\partial\mathbf{r}}\right). \quad (10)$$

In figure 1, the pictures of the density fields generated by a single lipid molecule (DPPC molecule) (bottom left) and the lipid bilayer assembly (top left) are depicted. Going from left to right the density resolution increases and at extreme right the particle models are depicted. In the figure, we report the main equations: the functional derivative giving the external potential (equation (6)), the definition of microscopic density (equation (2)) and the procedure with which the CG density $\phi(\mathbf{r})$ is given starting from particle positions (equation (11), given below). In the following the implementation of the MD-SCF approach, also for parallel computer architecture, will be reviewed.

3.2. Implementation

The MD algorithm (schematized in figure 2(*A*)) is implemented in the frame of particle–field approximations in the following way. The initial value of the external potential dependent on the density field is obtained from the initial configuration of the system (at time t_0). The potential energy is the sum of the intramolecular interaction potentials (bond, angles and other possible intramolecular interactions like dihedrals etc) and the external potential dependent on the density field. A new configuration is obtained by integrating the equation of motion of the particles from time t_0 to time $t_0 + \Delta t$ (in the practice case we used the velocity Verlet algorithm as implemented in OCCAM [59]). At every prefixed density update time ($\Delta t_{\mathrm{update}}$), the density is updated according to the positions of the particles in the simulation box. From the updated value of the density, a new value of the potential energy is calculated and then new forces are obtained. During the simulation the particle motions will contribute to a change in the spatial distribution of the density and this will cause a change in the density dependent self-consistent potential.

$$\tilde{S}\{\hat{\phi}(\mathbf{r};\Gamma)\} = \phi(\mathbf{r}). \quad (11)$$

From a technical point of view, the most relevant part of the theoretical framework described in the previous section is the way to obtain a smooth CG density function $\phi(\mathbf{r})$ from the particle positions Γ. This procedure is symbolically denoted in equation (11) and reported in figure 2. According to this procedure, first the simulation box is divided into several subcells and according to the positions of the particles in each of the simulation boxes, they are distributed among these cells. The values of the density field at the mesh points (vertices of the subcells) are defined by assigning fractions of each particle to its neighboring sub cell mesh point, according to the distances from the particle to the mesh point (see figure 2(*B*)). In this way the density function $\phi(\mathbf{r})$ is defined on a three-dimensional lattice and spatial derivatives of the density fields used for the calculation of the forces (equation (10)) are

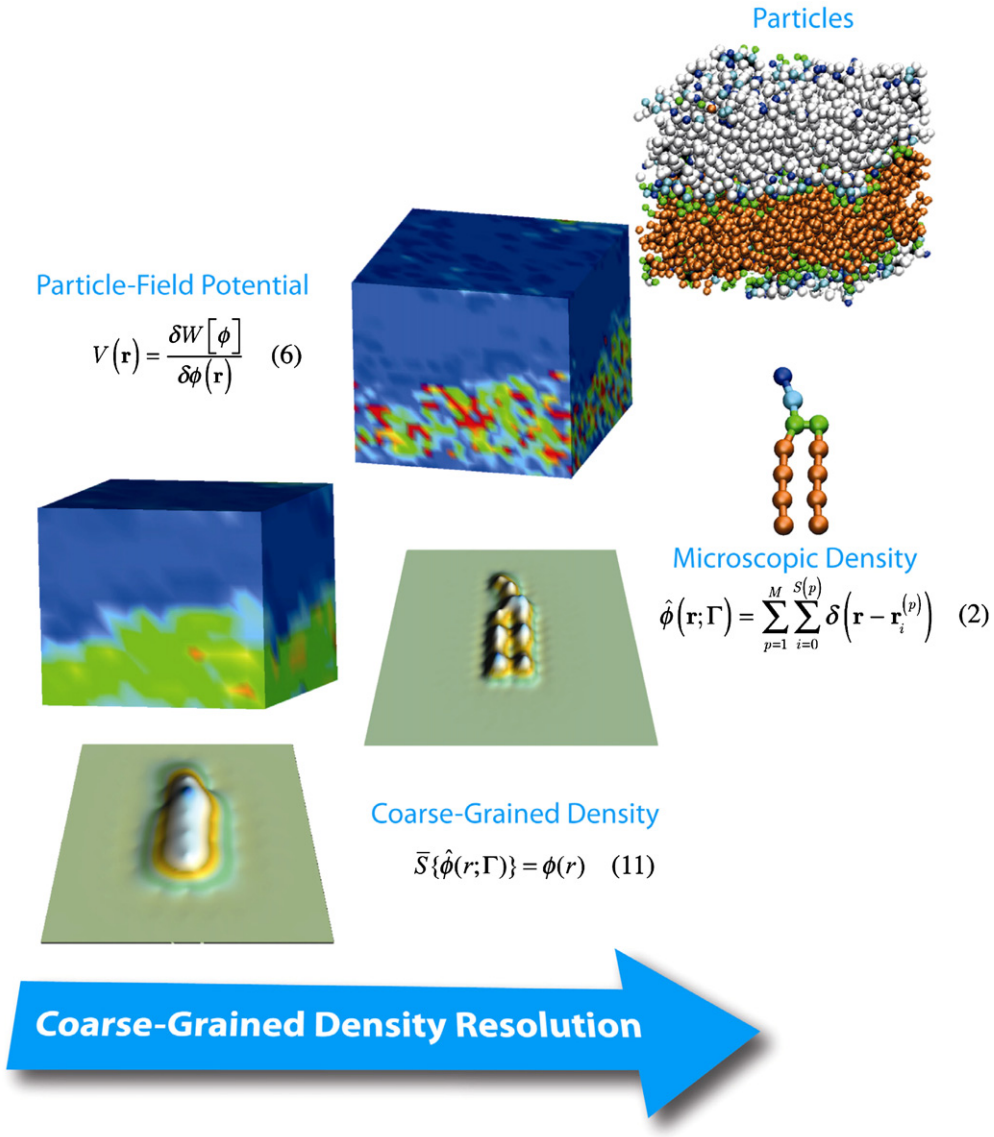

Figure 1. Graphical representation of the density field originating from a single DPPC molecule and a bilayer assembly.

obtained on a lattice staggered with respect to that for $\phi(\mathbf{r})$. During the simulations, the values of the density function and its derivatives are evaluated at position $\mathbf{r}$ between lattice points using linear interpolation of the values at neighboring lattice points.

It is worth noting that the most time consuming part of the simulation (i.e. the evaluation of intermolecular forces calculated in a double loop over particle pairs) has been skipped completely; it is replaced by an evaluation of a particle–field interaction term originating from the interaction of individual molecules with the density field $\phi(\mathbf{r})$. Furthermore, due to the CG nature of a collective field, it is possible to fix a time interval update without loss of accuracy. This choice is in agreement with the concepts behind the quasi-instantaneous field approximation discussed by Daoulas *et al* in the framework of SCMF Monte Carlo simulations [51]. The main assumption is that the field, as a collective variable with respect to particle coordinates, has a slow change with respect to a particle's displacement in one or more time-steps. In this way, in MD-SCF simulations there are two time-steps. The first '*microscopic time-step*' is the usual one for the particle's displacement used in MD simulations and the second '*mesoscopic time-step*' is for the field update. The quasi-instantaneous field approximation can be compared with methods using different time-integration steps for 'stiff' and 'soft' degrees of freedom, albeit not in the context of a field-theoretical representation of interactions. A popular example of this is MD algorithms with multiple time scales, introduced by Tuckerman *et al* [60]. The optimal value of the updated frequency depends on the density resolution (i.e. the size of the subcell where the particles are grouped), the system's nature and its conditions. For the systems considered here and reported in [54, 55, 61–63], we found that the value of Δt_{update} of the order of 100 time-steps gives accurate enough results (this aspect will also be considered in section 4). This approximation is relevant to enhance the computational performance, especially in parallel applications. This point will be discussed in more detail in the next section.

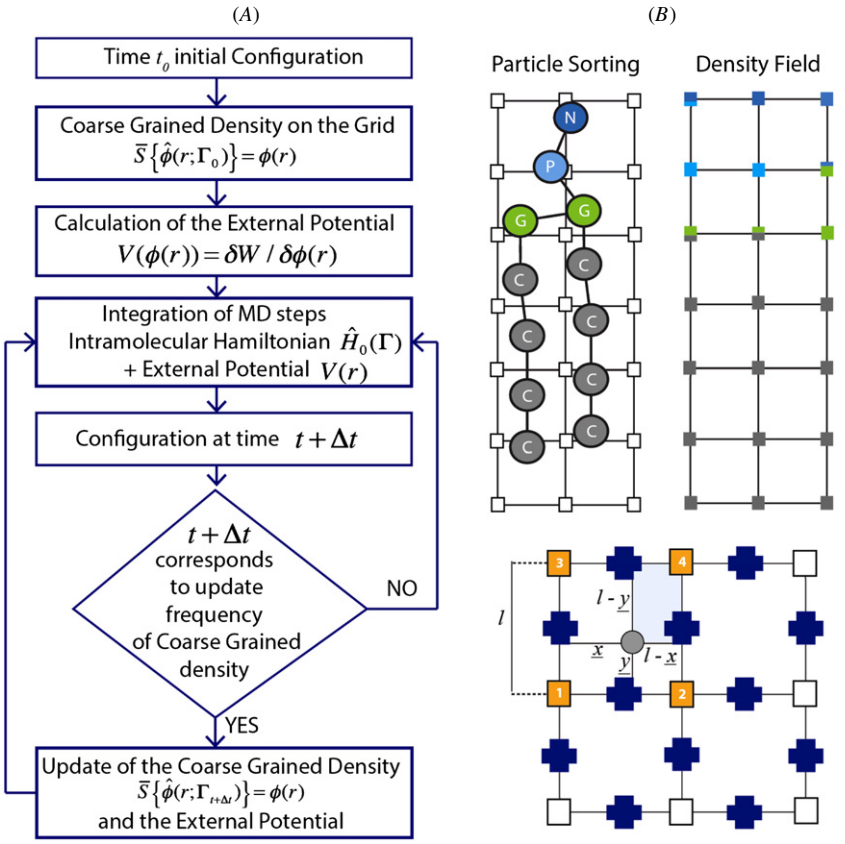

Figure 2. (*A*) Work flow chart of the iteration scheme for hybrid MD-SCF simulations. (*B*) Assignment of coarse-grained density to the lattice points for a phospholipid (top). Criterion for assignment of a particle fraction to lattice points (down).

3.3. Pressure calculation

The calculation of pressure profiles and the implementation of tensionless simulations are important ingredients of lipids models. The first step towards this is the calculation of the stress tensor for a hybrid particle–field Hamiltonian, which is not a trivial task. Only recently has a general formulation for the calculation of instantaneous pressure and the stress tensor in MD-SCF simulations been developed [55]. Recently, Kremer and Daoulas implemented a 'volume-changing' move used in NPT simulations of standard potential-based models [64] for this kind of hybrid particle–field simulation.

The scheme developed for MD-SCF simulations is derived from the statistical mechanical definition of the pressure. In particular, starting from the expression of the free energy functional obtained using the SCF theory for a melt consisting of M homopolymer molecules:

$$F[\phi(\mathbf{r})] = -k_BT\ln z^M + W[\phi(\mathbf{r})] - \int \mathrm{d}\mathbf{r}\, V(\mathbf{r})\phi(\mathbf{r}) + k_BT(M\ln M - M). \tag{12}$$

In order to calculate the pressure tensor, a virtual displacement $\mathbf{r}' = \mathbf{r} + \mathbf{u}(\mathbf{r})$, which leads to a change in the volume element $\mathrm{d}\mathbf{r}' = \mathrm{d}\mathbf{r}(1 + \nabla\cdot\mathbf{u})$, can be considered. We then have the following expressions for ϕ and V in the coordinate $\mathbf{r}'$:

$$\phi'(\mathbf{r}') = \phi(\mathbf{r}) - \phi(\mathbf{r})(\nabla\cdot\mathbf{u}),$$
$$V'(\mathbf{r}') = V(\mathbf{r}) - V(\mathbf{r})(\nabla\cdot\mathbf{u}). \tag{13}$$

Considering the transformation of the first three terms of the free energy expression given above, it is possible to write the stress tensor. The fourth term is the mixing entropy of the molecules' centers of mass.. Because this mixing entropy is a constant, it is possible to neglect it. In this way, a general expression of the pressure tensor for a multi-component system is given by:

$$\Pi_{\alpha\beta} = \left\{ -Mk_BT\left\langle\left(1+\beta\sum_i V(\mathbf{r}_i)\right)\right\rangle - k_BT\frac{1}{2v}\left[\sum_{KK'}\chi_{KK'}\int \mathrm{d}\mathbf{r}(\phi_K(\mathbf{r})\phi_{K'}(\mathbf{r}))\right] + \frac{1}{2kv}\left[\int \mathrm{d}\mathbf{r}\left(1-\sum_K\phi(\mathbf{r})^2\right)\right] + \left[\frac{1}{v}\sum_K\int \mathrm{d}\mathbf{r}\phi_K(\mathbf{r})V_K(\mathbf{r})\right]\right\}\frac{1}{3}\delta_{\alpha\beta}. \tag{14}$$

An implementation of the derived formulation suitable for hybrid particle–field MD-SCF simulations can be obtained. In particular, by construction, the density field is a much slower variable than the positions of individual particles. For this reason, in the particle–field contribution to the pressure tensor (first addend of equation (14)), the density field is expanded around the atomic positions. By expanding the first term of equation (14) around the atomic positions, the following

contribution of the particle–field interactions to the pressure tensor can be obtained:

$$\Pi_{\alpha\beta} = k_B T \delta_{\alpha\beta} \Bigg\langle 1 + \sum_{i=1}^{N} \left[\chi\phi(\mathbf{r}_{i,0}) + \frac{\beta}{\kappa}(\phi(\mathbf{r}_{i,0}) - 1) \right] + \sum_{i=1}^{N} \left(\chi + \frac{\beta}{\kappa} \right) \sum_{\alpha} \frac{\partial \phi(\mathbf{r}_{i,0})}{\partial (\mathbf{r}_{i,0})_\alpha} (\Delta \mathbf{r}_i)_\alpha + \frac{1}{2} \sum_{i=1}^{N} \left(\chi + \frac{\beta}{\kappa} \right) \sum_{\alpha} \sum_{\beta} \frac{\partial^2 \phi(\mathbf{r}_{i,0})}{\partial (\mathbf{r}_{i,0})_\alpha \partial (\mathbf{r}_{i,0})_\beta} \times (\Delta \mathbf{r}_i)_\alpha (\Delta \mathbf{r}_i)_\beta \Bigg\rangle. \quad (15)$$

The zeroth order term in the diagonal components, i.e. $\sum_{i=1}^{N} [\chi\phi(\mathbf{r}_{i,0}) + \frac{\beta}{\kappa}(\phi(\mathbf{r}_{i,0}) - 1)] \equiv V_{PF}$, is the contribution from the total interaction energy between the particles and the field $V_{\mathrm{PF1}} \equiv \sum_{i=1}^{N} \chi\phi(\mathbf{r}_{i,0})$ and the contribution from the incompressibility condition $V_{\mathrm{PF2}} \equiv \sum_{i=1}^{N} \frac{\beta}{\kappa}(\phi(\mathbf{r}_{i,0}) - 1)$. The first order term in $\Delta\mathbf{r}_i$ of the above equation is the sum over all the particles due to the interaction with the field by the particle displacement. A series of test simulations on model systems have been reported comparing the calculated pressure with those obtained from standard MD simulations based on pair potentials [55]. The evaluation of both the zeroth and the first order terms of the pressure tensor only involves quantities that have already been calculated during a MD simulation (i.e. the total particle–field interaction energy and the forces due to the interaction between the particles and the density field). Thus, the calculation of the stress tensor does not imply any extra computational costs. This approach has been validated and compared against particle–particle simulations for simple test systems (homopolymer and block copolymer melts). In particular, in figure 3, the behavior of the pressure as a function of the density for a homopolymer melt is reported from [55].

In the framework of the scheme described above, the implementation of tensionless simulations is under development and will make it possible to evaluate bending stiffness, which measures the energetic cost per unit area due to local curvature [25, 65].

3.4. Parallelization scheme

A further way to achieve larger length and time scales in molecular simulations is the exploitation of parallel computer hardware. There are two main ways to achieve parallelization, depending on the features of parallel architectures, which are extensively applied for parallelizing MD algorithms: shared memory through OpenMP [66] and distributed memory through the MPI (message passing interface) [67]. In the framework of the model of distributed memory through the MPI, several strategies of parallelization of a MD simulation program have been reported [68–77]. The most straightforward way of affording this is to distribute a subgroup of molecules into each processor thereby fixing the chosen distribution for the duration of the simulation, which is called particle–(atom) decomposition. In figure 4(*A*), the main parallelization strategy is schematized. Molecules are distributed among processors, the density field calculation is operated in a parallel fashion

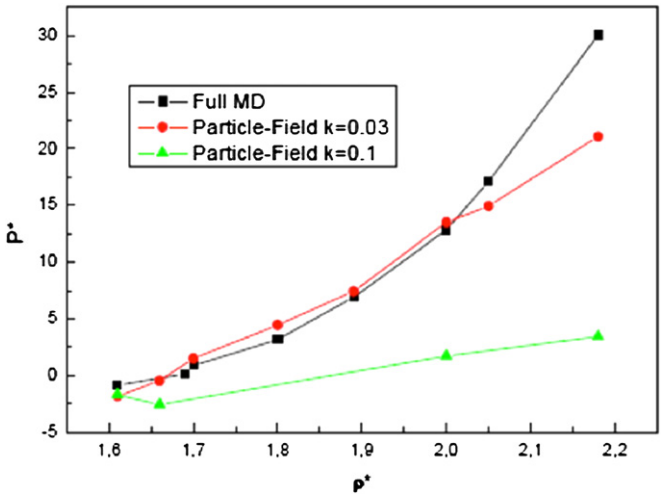

Figure 3. Comparison between particle–particle and particle–field models in the pressure calculation at different densities.

giving the partial densities calculated on each processor. A summation operation is operated when it is needed to update the density field. The latter is the only process in which communication between processors is needed.

Several benchmarks performed on the different systems show that the two main parameters (the density-update frequency and the size of the subcell) characterizing the density coarse-graining are very important in regulating the performances of parallel runs [78]. Considerable speedups have been achieved, especially when it is possible to update the density field with a low frequency. In figure 4(*B*), the benchmarks (number of steps/second) obtained by simulating a monoatomic fluid of 500 000 particles in comparison with the GROMACS code are reported. From the figure is clear that in all cases good performances can be obtained, especially when the update frequencies are larger than 100 time-steps.

In general, pure field models (not based on particles, only on SCF theory) are much less computationally expensive compared with particle based simulations. Typical applications of the pure SCF approach are simulations of block-copolymer mesophases with domain features on the 10 nm scale. A recent paper by Stasiaka and Matsen [79] examines the computational costs of SCF theory for the gyroid and spherical phases of diblock-copolymer melts. These calculations differ from molecular simulations as they typically need fewer iterations (from 20 to 100) to converge to equilibrium density fields. For these systems, an equilibrium density field can be obtained, using a 2.66 GHz Intel Xeon $\times$5650 processor, in a time duration from several seconds to 1 h, depending on the type of phase and the strength of phase separation. We recently performed particle–field simulations of similar systems of triblock copolymers in water [63]. To obtain equilibrium morphologies for these systems, usually simulations of the order of several μs have to be performed. To give a rough image of a comparison, a system with a box length of about 40 nm (consisting of 500 000 particles) has been considered. Using typical grid spacing and field update frequency (grid size 0.705 nm, field update every 300 steps), such a simulation can take about two days on 64 processors (2.33 GHz Intel

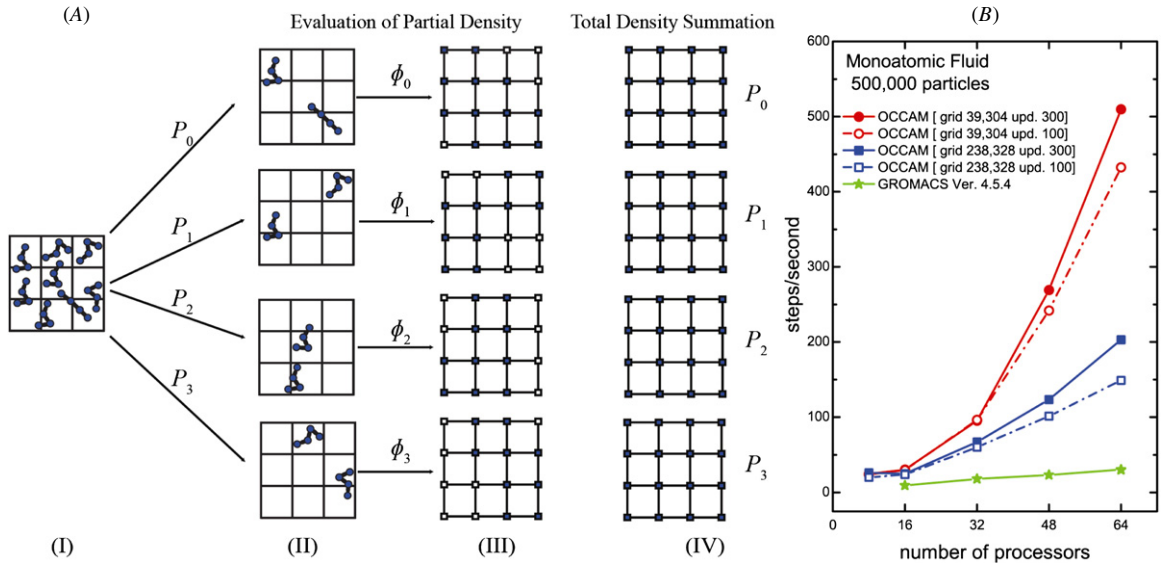

Figure 4. (*A*) Density-update parallelization strategy. An example of eight molecules assigned to four processors is shown. (I) System containing eight molecules in the three-dimensional box. (II) Partition of the eight molecules into four groups assigned to four different processors. (III) Calculation of the partial density on the vertices of subcells according to the positions of molecules. (IV) Total density is summed from the partial density of each processor. (*B*) Performances of parallel MD-SCF program as the step/s for monoatomic fluid system in comparison with GROMACS 4.5.4 (green curve). Results of OCCAM using 39 304 lattice points (red curves) and 238 328 lattice points (purple curves) are shown. Particle–field MD simulations have been done using update frequencies of 100 time-steps (empty symbols and dash-dot lines) and 300 time-steps (filled symbols and solid lines), respectively.

E5345). The ratio between the computational times for the particle–field approach to the standard MD simulations is a function of the system size and the number of processors employed. In particular, due to the low amount and less frequent data exchange, the larger the number of processors, the better the performance of the MD-SCF method. For instance, for the system reported in figure 4(*B*), the particle–field simulations can take from 40% (using 16 processors) to 12% (using 64 processors) of the CPU time needed for state-of-the art particle–particle simulations. In summary, to obtain equilibrium self-assembled morphologies for comparable systems with domain features on the 10 nm scale, pure SCF theory models need computation times of the order of seconds–hours whereas hybrid MD-SCF simulations take days and standard MD simulations take weeks. More details about parallel code performances and their implementation can be found in [78].

4. Simulation results of hybrid particle–field models of phospholipds

4.1. Description of models

As described in section 2, according to the formulation of hybrid MD-SCF models, the intramolecular bonded interactions (bond, angles, etc) can be described using traditional force fields that are suitable for molecular simulations. Our choice has been to develop a hybrid MD-SCF model based on the description that it is able to retain the chemical specificity. The coarse-graining scheme proposed by Marrink *et al* has been considered suitable for this purpose [61]. The advantages of these types of models, intermediate between atomistic and generic CG models, are that the parameterization of the interaction potentials is not tailored to a specific lipid and different phospholipids can be described from a small set of bead types. In figure 5(*A*), the coarse-graining mapping scheme and the underlying atomistic structures are exemplified for the phospholipid dipalmitoylphosphatidylcholine (DPPC).

Bond and angle interaction potentials, according to the formulation of the MD-SCF method, have the same functional form and parameters as those in the original MARTINI force field [30]. All non-bonded interactions are calculated using the assumption that each CG bead interacts with the density fields.

According to equation (8), in order to calculate the MD-SCF potential, several mean field parameters $\chi_{KK'}$ between a particle of type K with the density field due to particles of type K' are needed. A first value for these parameters can be obtained by following the Flory–Huggins approach for the calculation of χ parameters for lattice models:

$$\chi_{KK'} = \frac{z_{CN}}{k_B T}\left[\frac{2u_{KK'} - (u_{KK} + u_{KK'})}{2}\right], \qquad (16)$$

where $u_{KK'}$ is the pairwise interaction energy between a pair of adjacent lattice sites occupied by beads of types K and K'. These interaction energies can be set as $u_{KK'} = -\varepsilon_{KK'}$, where $\varepsilon_{KK'}$ are the Lennard-Jones ε parameters for the corresponding pairwise Lennard-Jones interactions. The coordination number z_{CN} in equation (16) takes the value 6 for a three-dimensional simple cubic lattice. For lipid molecules, the χ parameters obtained in this way have been found to be a good starting point; some refinements are needed to reproduce reference data [61]. Finally, in order to determine the value of the parameter κ, which

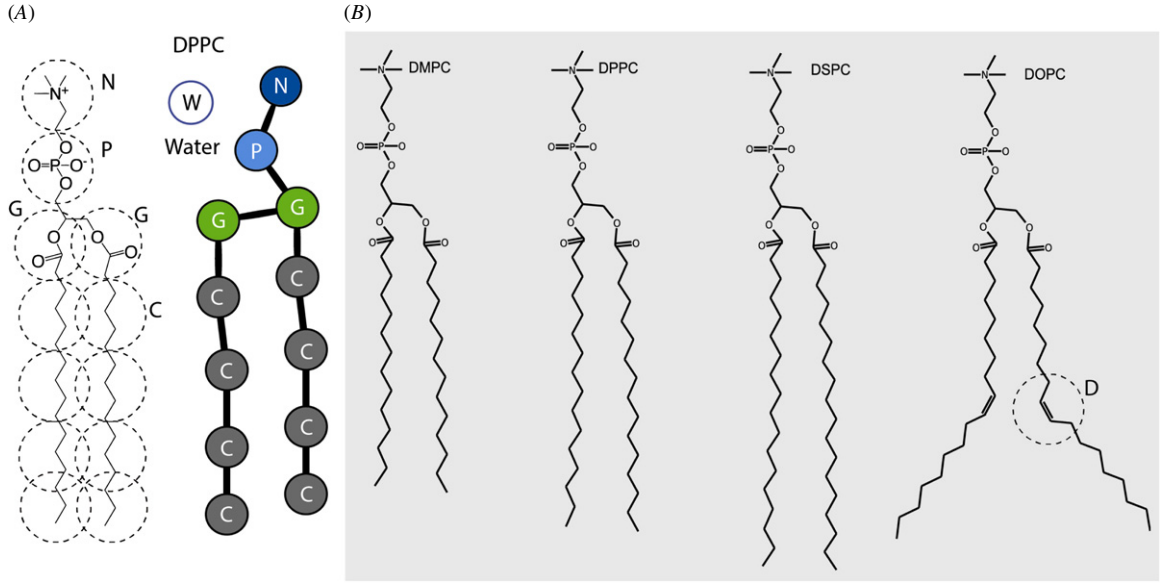

Figure 5. (*A*) Adopted CG scheme for the phospholipid DPPC. One CG bead corresponds to four atoms. (*B*) Chemical structures of the four phospholipids considered. For the DOPC phospholipid, the mapping for beads of type D, including carbon atoms involved in a double bond, is shown.

regulates the strength of the incompressibility condition imposed in equation (8), the behavior of density fluctuations in the reference MD simulations can be analyzed. This parameter then can be fixed to reproduce the behavior of the reference simulations. Furthermore, the choice of using χ parameters derived from particle–particle models showing thermodynamic consistency would also suggest reasonable thermodynamic behavior for the particle–field model. Of course this criterion is only indirect. The challenge of a good CG model is to obtain, as far as is possible, a reasonable description of both the structural and thermodynamic behavior. To have a full validation of the thermodynamics behavior, suitable free energy calculation protocols are needed for hybrid particle–field models. Extensive investigation involving free energy calculations, similar to the ones proposed in the literature to validate CG models in comparison with atomistic simulations [80], will further improve these particle–field models.

4.2. Lipid structures reproduction

Together with DPPC, the structures of three other different phospholipids are depicted in figure 5(*B*). In particular, three biologically relevant lipids, i.e. dimyristoylphosphatidylcholine (DMPC), distearoylphosphatidylcholine (DSPC) and dioleoylphosphatidylcholine (DOPC), are shown. Due to the straightforward way of representing the corresponding atomistic structure, tiny differences between the different lipids on the atomistic level can be taken into account. For the lipids depicted in figure 4, the main difference between DMPC, DPPC and DSPC is in the numbers of carbon atoms present in the hydrophobic tails. In this case, at CG level the models differ only in the number of type C beads that form the tails, while the parameters for the non-bonded, bond and angle potentials are the same. The presence of a double bond in the case of DOPC requires an extra particle type corresponding to four atoms including a double bond (see figure 5(*B*), type D bead).

In figure 6, the total electron density profiles obtained from the particle–field models calculated and from experiments are compared (part A). In the bottom part of the figure (part B), the partial density profiles are also reported. Together with the results of the particle–field simulations, in the top row of figure 6(*B*), the results obtained using classical MD simulations based on pair-wise potentials (particle–particle) are reported.

From the picture it is clear that the data obtained from simulations agree well with the experimental ones. From a more quantitative point of view, partial electron density profiles and the bilayer thickness (D_{HH}) can be calculated and compared with those of the reference MD simulations and available experimental data [81–83]. Although differences between the structures of the considered lipids are not big in terms of bilayer thickness, the reproduction of experimental D_{HH} values is surprisingly good. In particular, the calculated value for DPPC of 3.5 nm (particle–particle value 3.5 nm) is coincident with the experimental one; for DMPC the value of 3.7 nm (particle–particle value 3.7 nm) compares well with values between 3.8 and 3.5 nm reported in the literature [84]. For DOPC, the value of 4.0 nm (particle–particle value 4.1 nm) for the calculated density profiles is in fair agreement with 3.7–3.6 nm reported in the literature [84]; for DSPC, the calculated value of 4.4 nm (the largest one among the considered lipids, the particle–particle value is 4.1 nm) corresponds to the value between 4.0 and 4.1 nm reported in the literature [83, 84].

In order to understand the quality of the results as a function of the frequency update of the field, it is useful to use the particles' mean square displacement (MSD) as a function of time. In the figure below, the behavior of the square root of the MSD for water and the DPPC in units of cell length as a function of time for different values of update

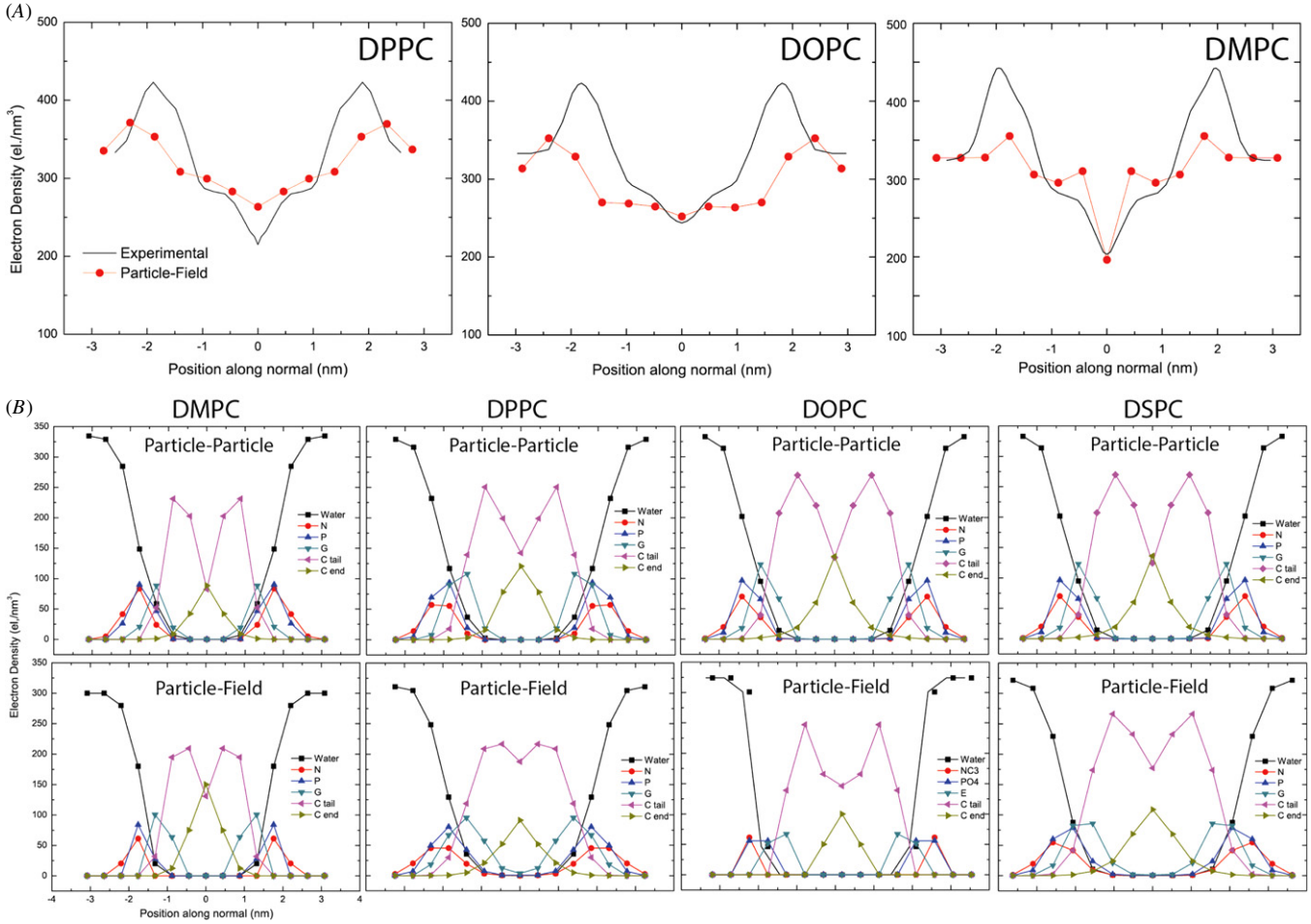

Figure 6. (*A*) Total electron density profiles, calculated and experimental, for DPPC, DOPC and DMPC. (*B*) Comparison between particle–particle and particle–field electron density distributions calculated for different phospholipids, respectively: DMPC, DPPC, DOPC and DSPC.

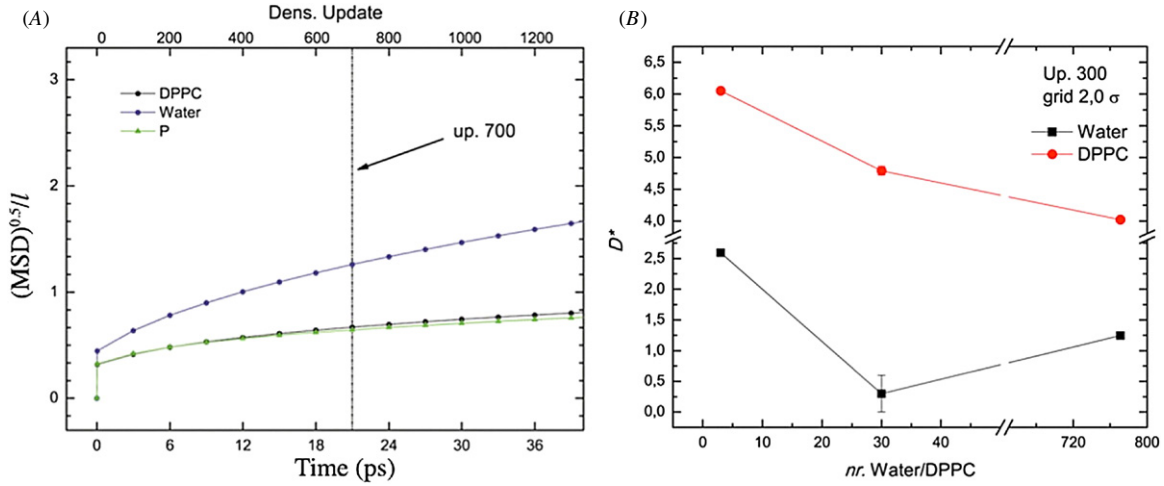

Figure 7. (*A*) Normalized mean square displacement (MSD) for water, DPPC and P beads as a function of time. (*B*) Scaling factor obtained for lipid–water mixtures at different water concentrations.

frequencies, is reported from [62]. In this way, it is possible to understand in a more quantitative way the validity of the quasi-instantaneous field approximation for our models. The plot of figure 7 quantifies how many cells a particle can cross in a given amount of simulation time. For update frequencies between 500 and 700 steps (corresponding to 15 and 21 ps) both water and DPPC beads have a displacement smaller than or equal to the cell size. These results are consistent with the

good reproduction of density profiles and bilayer thickness for update frequencies smaller than 700 steps.

Grouping several atoms in one effective bead determines the length scaling between the CG and the underlying atomistic model. For the models considered in this review, two additional coarse-graining parameters are connected with the representation of the field using particle positions. In particular, we have one length scale, i.e. the grid size l, and one time scale, i.e. the Δt between two density fields updates. For CG models, usually, the dynamics is faster because there is a reduced effective bead friction due to the smaller energy barriers and/or a smoother energy landscape. In order to connect the results with less coarse models (atomistic or CG but based on particle–particle potentials) or with experiments, it is necessary to connect the time-step used in CG simulations and to derive a scaling factor for the time. For dynamics, in general, the link between the time scales of the microscopic reference system and of the coarse system cannot be derived directly from the mapping scheme. A good overview of this important aspect of multiscale simulations has recently been published by Kremer *et al* as a perspective paper [85]. In the multiscale modeling literature, a few attempts have been reported to try a rigorous mapping of the dynamics of related CG and atomistic models. The main idea is to identify optimal reaction or transition pathways, which govern the time development of the systems, and form a comparison between the atomistic and CG models to obtain the scaling factor. In this direction, Depa and Maranas considered the escape of an atom from one local cage of nearest neighbors to another as an event, to which they apply the arguments derived from the hyper-MD method [86, 87]. These approaches are possible only for simple models, while the complications in soft matter systems are the multitude of fluctuating energy barriers of similar height; a common problem is that usually all barriers are not lowered in the exact same way so that the ratios of transition times remain the same [85].

More pragmatic methods to match time scales have been applied to quantitatively understand and predict the dynamics of several systems by CG models using a comparison between the dynamical properties calculated at the CG and atomistic level. In particular, time mapping between CG and atomistic simulations, based on the MSD of the center of mass of the chain for two different molecular weights of polystyrene, has been used to calculate in a quantitative way diffusion coefficients that are comparable with experiments for polymer melts also in the entangled regime [85, 88, 89].

Using the same approach, the dynamics of the reviewed CG models have been compared in a detailed way with corresponding particle–particle models. In particular, diffusion behavior has been compared as a function of both grid size l and field update Δt at different compositions. Comparisons between diffusion coefficients calculated using MD-SCF and classical MD based on Marrink models give a faster dynamics of the particle–field models; an example of a quantitative comparison is reported in figure 7(*B*). Interestingly, the ratio between $D_{\text{particle–field}}/D_{\text{particle–particle}} = D^*$ is a function of the composition. In figure 7(*B*), the behavior of the D^* function of the water content is reported. The scaling factor is different for the two components for the same system and is different at different concentrations. Similar behavior has been found by comparing the diffusion coefficients of multicomponent systems obtained from all atom and CG models of mixtures of ethylbenzene and polystyrene [90], lipids [91, 92] and ionic liquids [93].

Another important point to consider is the ability of the CG model to reproduce the correct phase at different conditions. In principle, the χ and κ parameters used in particle–field models are composition dependent. As the dependence on temperature is unknown, it can be different for different models and needs to be investigated. In particular, although the MARTINI force field, having an analogous mapping scheme, was shown to work very well for different mixtures of lipid bilayers [94, 95], the correct behavior of particle–field models, due to the further coarse-graining of a field representation, needs to be investigated.

This is a general problem of the statistical mechanics of coarse-graining procedures [96]. A comparison with simpler Landau–Ginzburg Hamiltonians developed for magnetic systems would probably make this point clearer. In principle, all the thermodynamic properties of a system can be calculated from a partition function obtained by summing the Boltzmann weights over all possible configurations of the degrees of freedom:

$$Z(T) = \text{tr}[\text{e}^{-\beta H_{\text{mic}}}]. \tag{17}$$

Now, let us change the focus from microscopic to mesoscopic scales. This scale is much larger than atomic lattice spacing, but much smaller than the system size. In a similar way to how we defined the density field $\phi(\mathbf{r})$ in our model, so too is it possible to define a magnetization field $\vec{m}(\mathbf{r})$. This field is the average of the elementary spins in the vicinity of a point $\mathbf{r}$. It is possible to obtain the transformation from the original microscopic degrees of freedom to the field variables by transforming the original microscopic probabilities arising from the Boltzmann weight $\text{e}^{-\beta H_{\text{mic}}}$.

The partition function is preserved in the coarse-graining process and can be written as:

$$Z(T) = \text{tr}[\text{e}^{-\beta H_{\text{mic}}}] \equiv \int D\vec{m}(\mathbf{r}) W[\vec{m}(\mathbf{r})] \tag{18}$$

where $D\vec{m}(\mathbf{r})$ indicates integration over all allowed configurations of the field. The different configurations of the field are weighted with a probability $W[\vec{m}(\mathbf{r})]$. This probability is what we need to find.

Using the CG weight, an effective Hamiltonian can be defined

$$\beta H[\vec{m}(\mathbf{r})] = -\ln W[\vec{m}(\mathbf{r})]. \tag{19}$$

The construction of the effective Hamiltonian makes use of several principles, i.e. locality, uniformity, analyticity, polynomial expansion and symmetry. It is possible to show that to describe magnetic systems it is sufficient to include only a few terms in the effective Hamiltonian leading to the so called Landau–Ginzburg Hamiltonian:

$$\beta H = \beta F_0 + \int \text{d}^d\mathbf{r} \left[\frac{t}{2} m^2(\mathbf{r}) + u m^4(\mathbf{r}) + \frac{K}{2} (\nabla m)^2 + \cdots - \vec{h} \cdot \vec{m}(\mathbf{r}) \right]. \tag{20}$$

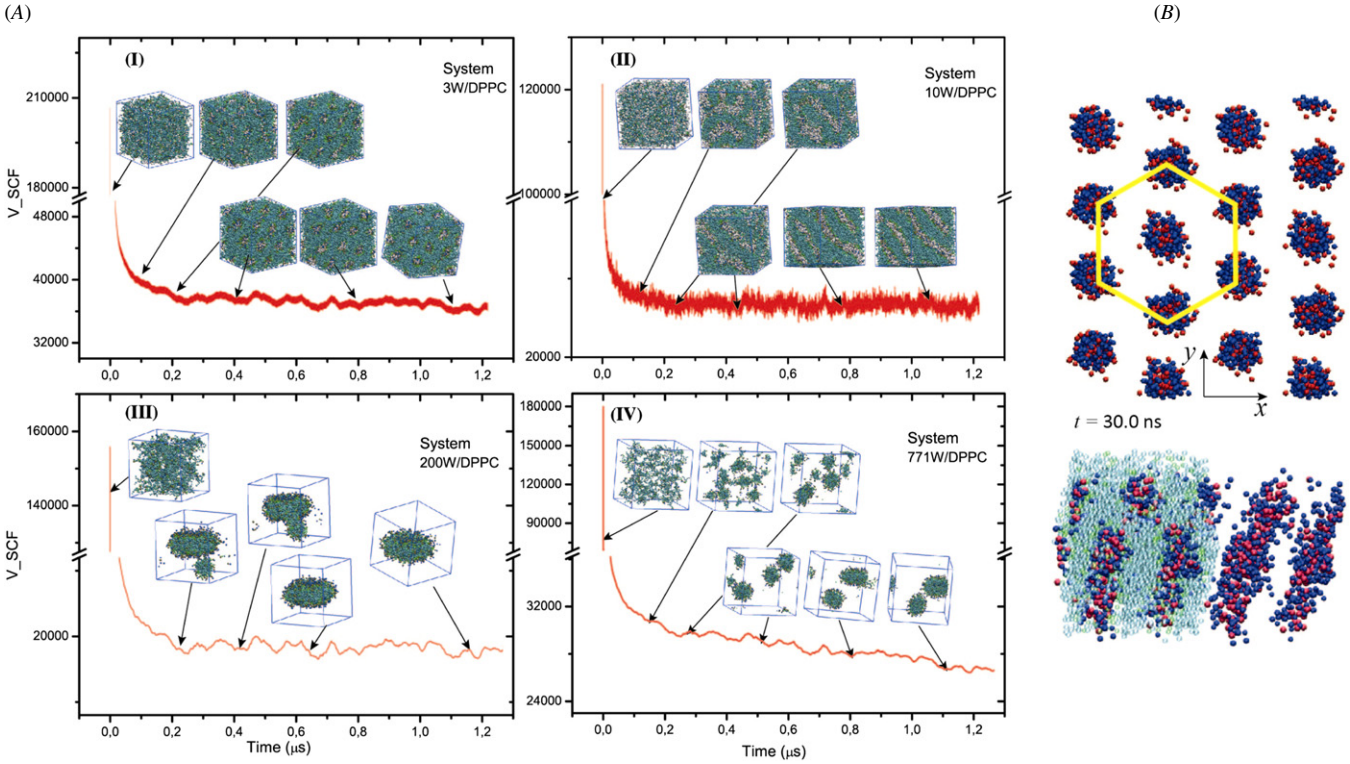

Figure 8. (*A*) Time behavior of the MD-SCF potential. In addition some representative snapshots are shown for each system. (I) System forming a reverse micellar hexagonal phase, (II) system forming a lipid bilayer phase, (III) system forming a single bicelle and (IV) system forming a micellar phase. (*B*) Detail of system (I) showing the hexagonal arrangement of cylindrical water channels in the reverse micellar phase.

The last term of the equation is the contribution from the magnetic work, where $\vec{h} \equiv \beta\vec{B}$ and $\vec{B}$ is the magnetic field. It is important to stress that, since it originates from a well defined physical system, the CG Boltzmann weight cannot lead to any unphysical field configuration. This implies, for instance, that the coefficient u in the equation above should be positive to avoid the fact that the probability diverges for infinitely large values of $\vec{m}$. There are also similar constraints for the sign of terms involving gradients to avoid oscillatory instabilities. Another important point is that the parameters t, u, K etc are phenomenological parameters; they are non-universal functions of microscopic interactions and external parameters, such as temperature and pressure. In fact, we have to account for the entropy of short distance fluctuations that have been lost in the coarse-graining process. These simple Hamiltonians are able to reproduce many structures observed in lipid–water mixtures like microemulsions but also more complicated periodic phases like the gyroid morphology [97, 98]; however, similar descriptions of biological systems are usually only qualitative.

In the case of the models reviewed here, the equivalent of the mesoscopic coefficients used to describe the intermolecular interactions can be compared with χ and κ parameters. The dependence of the parameters on the temperature and composition is not known *a priori* and needs to be investigated for every CG model. This is an important aspect because phospholipids show a rich variety of phase structures at different water compositions. They can form non-lamellar phases including the hexagonal and cubic phases, as well as the diluted micellar phases. Hexagonal phases are tubular aggregates and they can be composed either by normal or reverse aggregates. Cubic phases are composed of curved bilayers or micelles. Depending on the water concentration, micelles change their aggregation form from normal ('oil in water') to reverse ('water in oil') micelles. Test simulations have shown the ability of the model in the correct reproduction of non-lamellar phases. In particular, by varying the water content, particle–field models are able to correctly describe the different morphologies that are experimentally observed, such as micelles and reverse micelles.

Figure 8 summarizes the results reported in [62]. In particular, in figure 8(*A*) snapshots showing the spontaneous assembly of reverse micelles, lipid bilayers, bicelle and micelles going from a low to high water content, have been obtained. Furthermore, for the system at lower water content it has been possible to observe, in agreement with experiments, the hexagonal packing of tubular aggregates. The formation of these aggregates is clearer from figure 8(*B*).

The results of the investigation of DPPC at different water concentrations, in comparison with experiments and reference particle–particle simulations, indicate that the same constant χ parameter can be employed for different compositions. Such a model, although initially developed at water concentrations typical of lipid bilayers, can capture the different phases obtained for lipids at low (reverse micelle) and high (micelles) water concentrations. We want to stress that the models are not implicit solvent models, all the particles are there, but

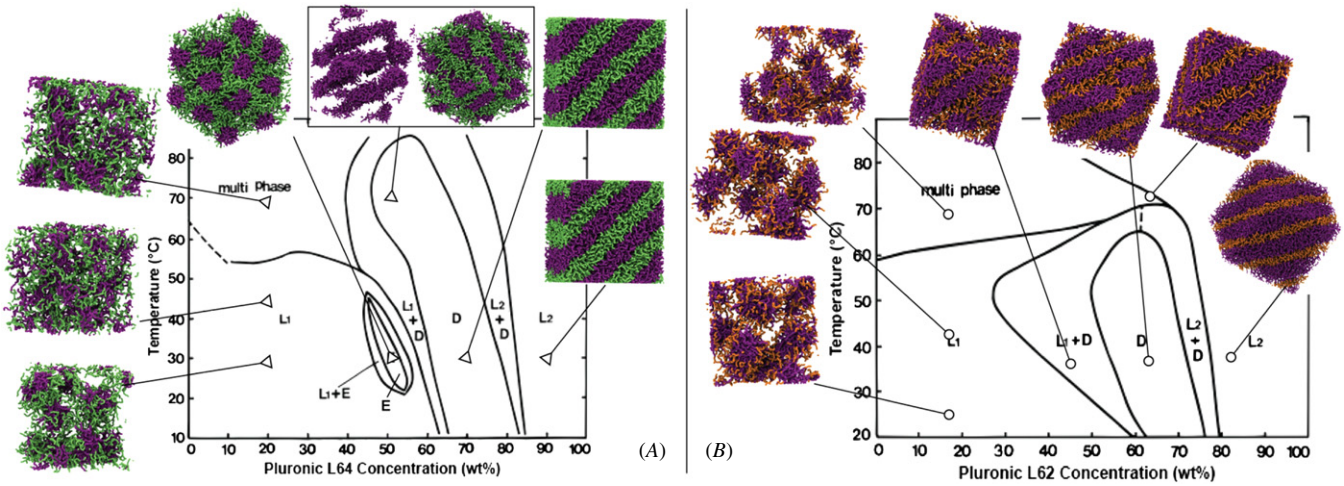

Figure 9. Phase diagram for Pluronics (*A*) L64 and (*B*) L62. A snapshot of the obtained morphology has been depicted on the diagram for each composition and temperature studied.

the interactions between them are calculated using on the fly computed density fields. In this way, different concentrations can be modeled in a straightforward way, just like for usual particle based models.

It is worth mentioning that similar results have also been obtained for a different system; in particular, very recently we studied mixtures of different triblock-copolymers with water at different concentrations [63]. In particular, the behavior of the models in the correct reproduction of micellar and non-micellar phases has been tested for Pluronic L62 and L64. The phase behaviour of the particle–field models is summarized in figure 9. At different polymer contents of the water/polymer mixtures, the proposed model is able to correctly describe the different morphologies that are experimentally found. Furthermore, the reproduction of the hexagonal morphology specific to Pluronic L64 has been obtained, in agreement with experiments for L64 but not for L62. Some of the equilibrium structures obtained using the MD-SCF simulations of L64 and L62 Pluronics are reported in the figure above. Although the two copolymers are very similar, a hexagonal phase is stable only in the case of L64 in a limited region of the phase diagram. As for temperature dependence, different behavior for our model with respect to the average number of Pluronics chains/cluster decreases with increasing temperature. The origin of this disagreement between experiments and simulations can be ascribed to the use of fixed $\chi_{KK'}$ parameters for different temperatures. A better agreement can be obtained using a more flexible model allowing the correct temperature dependence of the type $\chi = \chi_0(A + \frac{B}{T})$, where χ_0, A and B can be tuned to reproduce the correct experimental behavior.

Conclusions

The particle–field molecular dynamics method and its application to phoshpolipids have been reviewed. In particular, the description of the coarse-grained models, their validation in the reproduction of lipid bilayer structrures and the phase behavior as a function of water content have been given. For these models, the use of the mean field does not correspond to a truly field-based method or just particle–field coexistence; the density field remains a close function of the particle coordinates and is not an independent variable in the free energy functional. In the hybrid MD-SCF simulation all the particles are there; in other words, the particle coordinates are still the underlying dynamic variables and dictate the evolution of the system, i.e. the meshed density field is only a byproduct and is calculated on the fly from particle coordinates. For these reasons, the models described show enough flexibility in the description of different lipids and although they are coarse-grained they are still able to discriminate different chemistry. The computational efficiency of the particle–field method allows us to access large time and length scales but, at the same time, without loss of the chemical specificity. This feature makes these models very promising in the exploration of several problems in biophysics. Several applications related to drug delivery as well as protein adsorption on bilayer interfaces are currently being studied.

References

[1] van Gunsteren W F *et al* 2006 Biomolecular modeling: goals, problems, perspectives *Angew. Chem., Int. Edn. Engl.* **45** 4064–92
[2] Lee E H, Hsin J, Sotomayor M, Comellas G and Schulten K 2009 Discovery through the computational microscope *Structure* **17** 1295–306
[3] Monticelli L and Tieleman D P 2013 Force fields for classical molecular dynamics *Methods Mol. Biol.* **924** 197–213
[4] Sapay N and Tieleman D P 2008 Molecular dynamics simulation of lipid–protein interactions *Computational Modeling of Membrane Bilayers* ed S E Feller (*Current Topics in Membranes* vol 60) (New York: Academic) pp 111–30
[5] Lyubartsev A P and Rabinovich A L 2010 Recent development in computer simulations of lipid bilayers *Soft Matter* **7** 25
[6] Muller M, Katsov K and Schick M 2006 Biological and synthetic membranes: What can be learned from a coarse-grained description? *Phys. Rep.* **434** 113–76
[7] Riniker S, Allison J R and van Gunsteren W F 2012 On developing coarse-grained models for biomolecular simulation: a review *Phys. Chem. Chem. Phys.* **14** 12423

[8] Aisenbrey C, Bechinger B and Gröbner G 2008 Macromolecular crowding at membrane interfaces: adsorption and alignment of membrane peptides *J. Mol. Biol.* **375** 376–85

[9] Muller-Plathe F 2002 Coarse-graining in polymer simulation: from the atomistic to the mesoscopic scale and back *Chem. Phys. Chem.* **3** 754–69

[10] Loverde S M, Pantano D A, Christian D A, Mahmud A, Klein M L and Discher D E 2011 Curvature, rigidity, and pattern formation in functional polymer micelles and vesicles—from dynamic visualization to molecular simulation *Curr. Opin. Solid State Mater. Sci.* **15** 277–84

[11] Discher D E *et al* 2007 Emerging applications of polymersomes in delivery: from molecular dynamics to shrinkage of tumors *Prog. Polym. Sci.* **32** 838–57

[12] Marrink S J, de Vries A H and Tieleman D P 2009 Lipids on the move: simulations of membrane pores, domains, stalks and curves *Biochim. Biophys. Acta Biomembr.* **1788** 149–68

[13] Ayton G S and Voth G A 2009 Systematic multiscale simulation of membrane protein systems *Curr. Opin. Struct. Biol.* **19** 138–44

[14] Venturoli M, Sperotto M M, Kranenburg M and Smit B 2006 Mesoscopic models of biological membranes *Phys. Rep.* **437** 1–54

[15] Lyubartsev A P and Rabinovich A L 2011 Recent development in computer simulations of lipid bilayers *Soft Matter* **7** 25–39

[16] Peter C and Kremer K 2009 Multiscale simulation of soft matter systems—from the atomistic to the coarse-grained level and back *Soft Matter* **5** 4357–66

[17] Murtola T, Bunker A, Vattulainen I, Deserno M and Karttunen M 2009 Multiscale modeling of emergent materials: biological and soft matter *Phys. Chem. Chem. Phys.* **11** 1869–92

[18] Smit B, Hilbers P A J, Esselink K, Rupert L A M, van Os N M and Schlijper A G 1990 Computer simulations of a water/oil interface in the presence of micelles *Nature* **348** 624–5

[19] Sintes T and Baumgaertner A 1998 Interaction of wedge-shaped proteins in flat bilayer membranes *J. Phys. Chem.* B **102** 7050–7

[20] Sintes T and Baumgartner A 1997 Protein attraction in membranes induced by lipid fluctuations *Biophys. J.* **73** 2251–9

[21] Lenz O and Schmid F 2005 A simple computer model for liquid lipid bilayers *J. Mol. Liq.* **117** 147–52

[22] Goetz R and Lipowsky R 1998 Computer simulations of bilayer membranes: self-assembly and interfacial tension *J. Chem. Phys.* **108** 7397–409

[23] Shelley J C, Shelley M Y, Reeder R C, Bandyopadhyay S and Klein M L 2001 A coarse grain model for phospholipid simulations *J. Phys. Chem.* B **105** 4464–70

[24] Lyubartsev A P 2005 Multiscale modeling of lipids and lipid bilayers *Eur. Biophys. J. Biophys. Lett.* **35** 53–61

[25] Cooke I A and Deserno M 2005 Solvent-free model for self-assembling fluid bilayer membranes: stabilization of the fluid phase based on broad attractive tail potentials *J. Chem. Phys.* **123** 224710

[26] Venturoli M, Smit B and Sperotto M M 2005 Simulation studies of protein-induced bilayer deformations, and lipid-induced protein tilting, on a mesoscopic model for lipid bilayers with embedded proteins *Biophys. J.* **88** 1778–98

[27] Izvekov S and Voth G A 2006 Multiscale coarse-graining of mixed phospholipid/cholesterol bilayers *J. Chem. Theory Comput.* **2** 637–48

[28] Orsi M, Haubertin D Y, Sanderson W E and Essex J W 2008 A quantitative coarse-grain model for lipid bilayers *J. Phys. Chem.* B **112** 802–15

[29] Wang Z J and Deserno M 2010 Systematic implicit solvent coarse-graining of bilayer membranes: lipid and phase transferability of the force field *New J. Phys.* **12** 095004

[30] Marrink S J, de Vries A H and Mark A E 2003 Coarse grained model for semiquantitative lipid simulations *J. Phys. Chem.* B **108** 750–60

[31] Faller R and Marrink S-J 2004 Simulation of domain formation in DLPC–DSPC mixed bilayers *Langmuir* **20** 7686–93

[32] Marrink S-J and Mark A E 2004 Molecular view of hexagonal phase formation in phospholipid membranes *Biophys. J.* **87** 3894–900

[33] Marrink S J and Mark A E 2003 Molecular dynamics simulation of the formation, structure, and dynamics of small phospholipid vesicles *J. Am. Chem. Soc.* **125** 15233–42

[34] Dickey A N and Faller R 2005 Investigating interactions of biomembranes and alcohols: a multiscale approach *J. Polym. Sci.* B **43** 1025–32

[35] Notman R, Noro M, O'Malley B and Anwar J 2006 Molecular basis for dimethylsulfoxide (DMSO) action on lipid membranes *J. Am. Chem. Soc.* **128** 13982–3

[36] Lee H and Larson R G 2006 Molecular dynamics simulations of PAMAM dendrimer-induced pore formation in DPPC bilayers with a coarse-grained model *J. Phys. Chem.* B **110** 18204–11

[37] Monticelli L, Kandasamy S K, Periole X, Larson R G, Tieleman D P and Marrink S J 2008 The MARTINI coarse-grained force field: extension to proteins *J. Chem. Theory Comput.* **4** 819–34

[38] Kawakatsu T 2004 *Statistical Physics of Polymers* (Berlin: Springer)

[39] Matsen M W and Schick M 1994 Stable and unstable phases of a diblock copolymer melt *Phys. Rev. Lett.* **72** 2660–3

[40] Drolet F and Fredrickson G H 1999 Combinatorial screening of complex block copolymer assembly with self-consistent field theory *Phys. Rev. Lett.* **83** 4317–20

[41] Fredrickson G H, Ganesan V and Drolet F 2002 Field-theoretic computer simulation methods for polymers and complex fluids *Macromolecules* **35** 16–39

[42] Lauw Y, Leermakers F A M and Stuart M A C 2006 Self-consistent-field analysis of the micellization of carboxy-modified poly(ethylene oxide)-poly(propylene oxide)-poly(ethylene oxide) triblock copolymers *J. Phys. Chem.* B **110** 465–77

[43] Dickinson E, Pinfield V J, Horne D S and Leermakers F A M 1997 Self-consistent-field modelling of adsorbed casein interaction between two protein-coated surfaces *J. Chem. Soc. Faraday Trans.* **93** 1785–90

[44] Balazs A C, Singh C and Zhulina E 1998 Modeling the interactions between polymers and clay surfaces through self-consistent field theory *Macromolecules* **31** 8370–81

[45] Roan J R and Kawakatsu T 2002 Self-consistent-field theory for interacting polymeric assemblies: I. Formulation, implementation, and benchmark tests *J. Chem. Phys.* **116** 7283–94

[46] Roan J R and Kawakatsu T 2002 Self-consistent-field theory for interacting polymeric assemblies: II. Steric stabilization of colloidal particles *J. Chem. Phys.* **116** 7295–310

[47] Marcelja S 1973 Molecular model for phase transition in biological membranes *Nature* **241** 451–3

[48] Leermakers F, Rabinovich A and Balabaev N 2003 Self-consistent-field modeling of hydrated unsaturated lipid bilayers in the liquid-crystal phase and comparison to molecular dynamics simulations *Phys. Rev.* E **67** 011910

[49] Muller M and Schick M 1998 Calculation of the phase behavior of lipids *Phys. Rev.* E **57** 6973

[50] Szleifer I and Carignano M A 2007 Tethered polymer layers *Advances in Chemical Physics* vol 94 (New York: Wiley) pp 165–260

[51] Daoulas K C and Muller M 2006 Single chain in mean field simulations: quasi-instantaneous field approximation and quantitative comparison with Monte Carlo simulations *J. Chem. Phys.* **125** 184904

[52] Daoulas K C, Muller M, de Pablo J J, Nealey P F and Smith G D 2006 Morphology of multi-component polymer systems: single chain in mean field simulation studies *Soft Matter* **2** 573–83

[53] Daoulas K C, Cavallo A, Shenhar R and Muller M 2009 Phase behaviour of quasi-block copolymers: a DFT-based Monte-Carlo study *Soft Matter* **5** 4499–509

[54] Milano G and Kawakatsu T 2009 Hybrid particle–field molecular dynamics simulations for dense polymer systems *J. Chem. Phys.* **130** 214106

[55] Milano G and Kawakatsu T 2010 Pressure calculation in hybrid particle–field simulations *J. Chem. Phys.* **133** 214102

[56] Homberg M and Muller M 2010 Main phase transition in lipid bilayers: phase coexistence and line tension in a soft, solvent-free, coarse-grained model *J. Chem. Phys.* **132** 155104

[57] Sevink G J A, Charlaganov M and Fraaije J G E M 2013 Coarse-grained hybrid simulation of liposomes *Soft Matter* **9** 2816–31

[58] Fredrickson G H 2005 *The Equilibrium Theory of Inhomogeneous Polymers* (Oxford: Oxford University Press)

[59] Milano G 2007 OCCAM 3.0. University of Salerno

[60] Tuckerman M E, Glenn J M and Bruce J B 1990 Molecular dynamics algorithm for condensed systems with multiple time scales *J. Chem. Phys.* **93** 5

[61] De Nicola A, Zhao Y, Kawakatsu T, Roccatano D and Milano G 2011 Hybrid particle–field coarse-grained models for biological phospholipids *J. Chem. Theory Comput.* **7** 2947–62

[62] De Nicola A, Zhao Y, Kawakatsu T, Roccatano D and Milano G 2012 Validation of a hybrid MD-SCF coarse-grained model for DPPC in non-lamellar phases *Theor. Chem. Acc.* **131** 1167

[63] De Nicola A, Milano G and Kawakatsu T 2013 A hybrid particle–field coarse-grained molecular model for pluronics water mixtures *Macromol. Chem. Phys.* at press

[64] Zhang G, Daoulas K C and Kremer K 2013 A new coarse grained particle-to-mesh scheme for modeling soft matter *Macromol. Chem. Phys.* **214** 214–24

[65] Lindahl E and Edholm O 2000 Mesoscopic undulations and thickness fluctuations in lipid bilayers from molecular dynamics simulations *Biophys. J.* **79** 426–33

[66] Dagum L and Menon R 1998 OpenMP: an industry standard API for shared-memory programming *IEEE Comput. Sci. Eng.* **5** 46–55

[67] Gropp W, Lusk E, Doss N and Skjellum A 1996 A high-performance portable implementation of the MPI message passing interface standard *Parellel Comput.* **22** 789–828

[68] Berendsen H J C, van der Spoel D and van Drunen R 1995 GROMACS: a message-passing parallel molecular dynamics implementation *Comput. Phys. Commun.* **91** 43–56

[69] Forester T R and Smith W 1995 DL_POLY User Manual CCLRC DLW, UK

[70] Stadler J, Mikulla R and Trebin H R 1997 IMD: a software package for molecular dynamics studies on parallel computers *Int. J. Mod. Phys.* C **8** 1131–40

[71] Lyubartsev A P and Laaksonen A 2000 M.DynaMix—a scalable portable parallel MD simulation package for arbitrary molecular mixtures *Comput. Phys. Commun.* **128** 565–89

[72] Couturier R and Chipot C 2000 Parallel molecular dynamics using OpenMP on a shared memory machine *Comput. Phys. Commun.* **124** 49–59

[73] Straatsma T P, Philippopoulos M and McCammon J A 2000 NWChem: exploiting parallelism in molecular simulations *Comput. Phys. Commun.* **128** 377–85

[74] Roy S, Jin R Y, Chaudhary V and Hase W L 2000 Parallel molecular dynamics simulations of alkane/hydroxylated α-aluminum oxide interfaces *Comput. Phys. Commun.* **128** 210–8

[75] Goedecker S 2002 Optimization and parallelization of a force field for silicon using OpenMP *Comput. Phys. Commun.* **148** 124–35

[76] Özdoğan C, Dereli G and Çağın T 2002 O(N) parallel tight binding molecular dynamics simulation of carbon nanotubes *Comput. Phys. Commun.* **148** 188–205

[77] FrantzDale B, Plimpton S and Shephard M 2010 Software components for parallel multiscale simulation: an example with LAMMPS *Eng. Comput.* **26** 205–11

[78] Zhao Y, De Nicola A, Kawakatsu T and Milano G 2012 Hybrid particle–field molecular dynamics simulations: parallelization and benchmarks *J. Comput. Chem.* **33** 868–80

[79] Stasiak P and Matsen M W 2011 Efficiency of pseudo-spectral algorithms with Anderson mixing for the SCFT of periodic block-copolymer phases *Eur. Phys. J.* E **34** 1–9

[80] Baron R, Trzesniak D, de Vries A H, Elsener A, Marrink S J and van Gunsteren W F 2007 Comparison of thermodynamic properties of coarse-grained and atomic-level simulation models *Chem. Phys. Chem.* **8** 452–61

[81] Katsaras J, Tristran-Nagle S, Liu Y, Headrick R L, Fontes E, Mason P C and Nagle J F 2000 Revisiting the ripple phase using fully hydrated, aligned DPPC multibilayers *Biophys. J.* **78** 116

[82] Nagle J F, Zhang R, Tristram-Nagle S, Sun W, Petrache H I and Suter R M 1996 X-ray structure determination of fully hydrated L alpha phase dipalmitoylphosphatidylcholine bilayers *Biophys. J.* **70** 1419–31

[83] Balgavı P, Dubniková M, Kuerka N, Kiselev M, Yaradaikin S and Uhríková D 2001 Bilayer thickness and lipid interface area in unilamellar extruded 1, 2-diacylphosphatidylcholine liposomes: a small-angle neutron scattering study *Biochim. Biophys. Acta Biomembr.* **1512** 40–52

[84] Nagle J F and Tristram-Nagle S 2000 Structure of lipid bilayers *Biochim. Biophys. Acta Rev. Biomembr.* **1469** 159–95

[85] Fritz D, Koschke K, Harmandaris V A, van der Vegt N F and Kremer K 2011 Multiscale modeling of soft matter: scaling of dynamics *Phys. Chem. Chem. Phys.* **13** 10412–20

[86] Depa P K and Maranas J K 2005 Speed up of dynamic observables in coarse-grained molecular-dynamics simulations of unentangled polymers *J. Chem. Phys.* **123** 094901

[87] Depa P K and Maranas J K 2007 Dynamic evolution in coarse-grained molecular dynamics simulations of polyethylene melts *J. Chem. Phys.* **126** 054903

[88] Auhl R, Everaers R, Grest G S, Kremer K and Plimpton S J 2003 Equilibration of long chain polymer melts in computer simulations *J. Chem. Phys.* **119** 12718–28

[89] Milano G and Muller-Plathe F 2005 Mapping atomistic simulations to mesoscopic models: a systematic coarse-graining procedure for vinyl polymer chains *J. Phys. Chem.* B **109** 18609–19

[90] Fritz D, Herbers C R, Kremer K and van der Vegt N F A 2009 Hierarchical modeling of polymer permeation *Soft Matter* **5** 4556–63

[91] Marrink S J, de Vries A H and Mark A E 2004 Coarse grained model for semiquantitative lipid simulations *J. Phys. Chem.* B **108** 750–60

[92] Thogersen L, Schiott B, Vosegaard T, Nielsen N C and Tajkhorshid E 2008 Peptide aggregation and pore formation in a lipid bilayer: a combined coarse-grained and all atom molecular dynamics study *Biophys. J.* **95** 4337–47

[93] Karimi-Varzaneh H A, Mueller-Plathe F, Balasubramanian S and Carbone P 2010 Studying long-time dynamics of imidazolium-based ionic liquids with a systematically coarse-grained model *Phys. Chem. Chem. Phys.* **12** 4714–24

[94] de Vries A H, Mark A E and Marrink S J 2004 The binary mixing behavior of phospholipids in a bilayer: a molecular dynamics study *J. Phys. Chem.* B **108** 2454–63

[95] Baron R, de Vries A H, Hünenberger P H and van Gunsteren W F 2006 Configurational entropies of lipids in pure and mixed bilayers from atomic-level and coarse-grained molecular dynamics simulations *J. Phys. Chem.* B **110** 15602–14

[96] Kardar M 2007 *Satistical Physics of Fields* (New York: Cambridge University Press)

[97] Gompper G and Kraus M 1993 Ginzburg–Landau theory of ternary amphiphilic systems: II. Monte Carlo simulations *Phys. Rev.* E **47** 4301–12

[98] Góźdź W T and Hołyst R 1996 Triply periodic surfaces and multiply continuous structures from the Landau model of microemulsions *Phys. Rev.* E **54** 5012–27